An Analysis of Planetary Helium

by Kris H. Green, University of Tennessee, Department of Physics
May 10, 1994

under the direction of Drs. Joerg Mueller and Joachim Burgdoerfer

I. Introduction

Classical mechanics is sufficient to analytically describe the motions of systems involving the interactions of two particles. However, the three-body problem cannot be completely solved analytically, due to its nonintegrability. It can, however, be solved numerically. Since there are numerous physical systems which can be described as a three-body interaction, such as planetary systems, the quarks inside a baryon, two electron systems, and one electron molecules, it is important to understand this problem.

The interactions of planetary bodies involve attractive gravitational forces, so that each body is attracted to each other body by a force which is inversely proportional to the square of the distance between the two bodies. Quark interactions take place through the strong force, which is proportional the distance between two particles, much like Hooke's law for springs. In each of these cases, and in many other, less physical examples, the forces involved have the same sign, so that the particles are all attracted towards each other in some fashion. However, these systems all exhibit instabilities under certain conditions.

There are many three-body systems, such as helium, which are more complex than this. Helium consists of two negatively charged electrons orbiting a positively charged alpha particle. The three particles interact through Coulombic forces, so that each electron is attracted to the alpha particle. The interactions between the two electrons are repulsive. Like other examples, the helium atom exhibits instabilities under certain conditions. This paper will attempt to identify some of the conditions under which the system remains stable.

The helium atom is a quantum mechanical system, and, as such, is subject to the laws of quantum mechanics. The methods of quantum mechanics are fully sufficient to understand the simplest atom, hydrogen. This atom is a simple two body system. Perturbation theory is necessary to describe the quantum mechanics of the helium atom. Thus, the helium atom can be used to study the classical mechanics of the three-body Coulomb problem as well as the quantum mechanics of such a system. Comparison between the two can be used to further the studies of both.

Studies of the classical mechanics of helium have led to the identification of several periodic orbits: the Wannier orbit, the Langmuir orbit, and the asymmetric stretch. Each of these involves the electrons being separated by the nucleus, as shown below. Of the three, only the Langmuir orbit is known to be stable. This paper will focus on a fourth type of orbit, the planetary orbits, so named because of their resemblance to their gravitational counterparts.

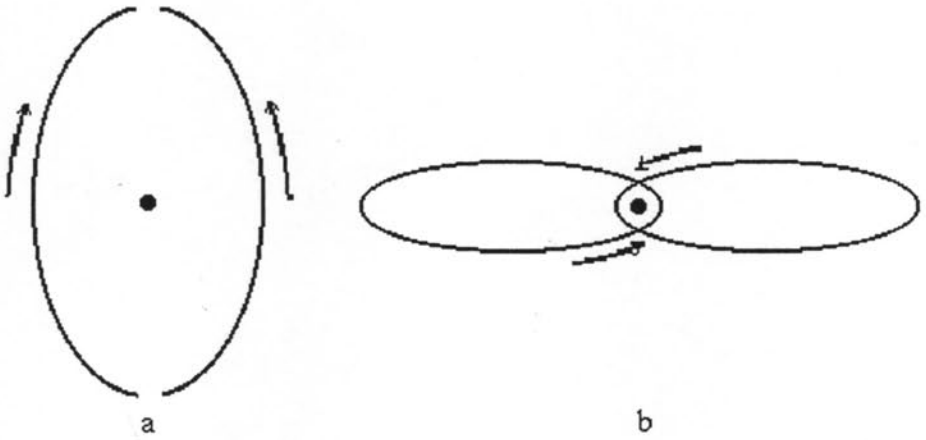


Figure 1. Illustration of the (a) Langmuir and (b) Wannier orbit.

A planetary orbit (classically) or planetary state (quantum mechanically) is an orbit/state in which both electrons are excited. Thus, neither lies at the lowest possible energy. Additionally, both are on the same side of the nucleus, one very far away and one much closer, so that it almost moves on a Keplerian ellipse.

II. Planetary Orbits

II.1 Mathematical Description

To begin studying the helium atom as a three-body problem, we first define coordinates for the system as shown below. By considering situations in which the total angular momentum is zero, we reduce the problem to motion in a plane. In general, each particle requires two spatial coordinates and two momentum coordinates, giving a system of twelve variables. The system can be reduced to eight variables if we further assume that the nucleus is massive enough that the forces acting on it can be neglected.

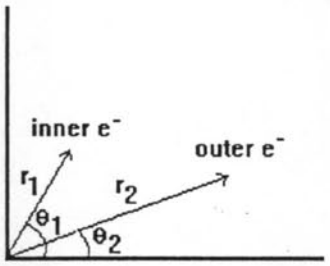


Figure 2. Illustration of the coordinate system.

The Hamiltonian (in Cartesian coordinates) for this system is

$$H = \frac{1}{2}\left(p_{x1}^2 + p_{y1}^2 + p_{x2}^2 + p_{y2}^2\right) - \frac{Z}{r_1} - \frac{Z}{r_2} + \frac{1}{r_{12}}$$

where the **r's** represent the radial distance to each electron, and the inter-electron distance. Z represents the total nuclear charge, which is two for helium. This Hamiltonian produces eight ordinary differential equations by application of the Hamiltonian equations

$$\dot{q}_i = \partial H / \partial p_i$$

$$\dot{p}_i = -\partial H / \partial q_i$$

which can be numerically integrated. The equations themselves have singularities when there is a collision between any two of the three particles (the electrons and the nucleus). However, by using the noncanonical transformations

$$x_1 = u^2 - v^2$$
$$y_1 = 2uv$$
$$p_{x1}^2 + p_{y1}^2 = \frac{1}{4}\left[\frac{p_u^2 + p_v^2}{u^2 + v^2}\right]$$

the equations can be partially regularized, removing the singularities. The new Hamiltonian is then

$$h = \frac{1}{2}\left(\frac{1}{4}\frac{p_u^2 + p_v^2}{u^2 + v^2} + p_{x2}^2 + p_{y2}^2\right) - \frac{Z}{u^2 + v^2} - \frac{Z}{r_2} + \frac{1}{R_{12}}$$

which again produces eight differential equations, two for each degree of freedom. This can be further improved by regularizing the time. The current method, when combined with a variable time step numeric integration process leads to an increase in energy conservation by a factor of about 30%. The time has not been regularized in the current scheme. These eight equations are coupled, making it impossible to derive an analytic solution, and forcing us to use numerical methods to calculate trajectories and lifetimes. Note that only the momenta and coordinates of one electron have been regularized. These are the position and momenta of the inner electron, the one closest to the nucleus.

In order to use numerical methods, we must first define the initial conditions for the system. It is convenient to use the hyperspherical coordinates (and their corresponding momenta)

$$R = \sqrt{r_1^2 + r_2^2} \qquad \alpha = \arctan\left(\frac{r_1}{r_2}\right) \qquad \Theta = \theta_1 - \theta_2$$

$$p_R = \dot{R} \qquad p_\alpha = R^2\dot{\alpha} \qquad p_\Theta = R^2\dot{\Theta}$$

in order to describe the six initial conditions needed. For planetary orbits, we start with both electrons initially on the same side of the nucleus, $\theta_{12}=0$. This reduces the number of initial conditions needed to specify the problem to only five. This can further be reduced by scaling the total energy to be constant at E=-1. Since the time derivative of θ can be related to the total energy once the other coordinates are known, we now only need four initial conditions to specify the problem: R, dR/dt, α, and $d\alpha/dt$. Even though only these four are needed, it is still a daunting task to search the phase

space for possibly stable orbits. Other methods than the "hit and miss" approach of guessing initial conditions are needed.

II.2 Trajectories for Helium (Z=2)

The problem has now been reduced to a four dimensional phase space in which we must search for initial conditions leading to stable and/or periodic orbits. What is needed is a systematic method for searching this phase space. By hit-and-miss guessing, we can examine trajectories of the two electrons in Cartesian space. The following page shows a typical planetary orbit, as well as the effects on the orbit of slightly altering the initial conditions.

It is seen that the inner electron travels on a nearly-precessing ellipse around the nucleus. We describe the path as "nearly-precessing" because the major axis of the ellipse is confined to a certain angular region, instead of sweeping all the way around the nucleus. It is also seen that the outer electron is confined both to an angular region and a radial region. The breaking up of this angular confinement inevitably leads to autoionization, a situation in which one, or both, of the electrons gains sufficient energy to escape the binding force of the nucleus.

Below (see figure 4) is an illustration of another trajectory. It is clear that this trajectory shows many of the same characteristics as the trajectory above. However, the outer electron is more confined, following a complex, winding path after a few increments of time. This orbit is characteristic of a "torus-filling" type of orbit. The inner electron also follows a much more regular path, with its Keplerian ellipse precessing symmetrically and the inner electron confined inside a definite region close to the nucleus. There is an apparent "wall" which this electron cannot pass.

Rather than using the full Hamiltonian of the system, one can use the frozen planetary approximation (FPA.) This model assumes that the outer electron's motion is negligible, and simply ignores it, freezing the electron in place. There is thus an electric field (that of a point charge) acting on the inner electron. This leads to the "nearly-precessing" ellipse; however, the motions of the inner electron are much more regular than when using the correct Hamiltonian. Later in this paper, it is shown that there is an additional flaw--all orbits are stable and periodic in the FPA, whereas the true Hamiltonian does not produce such regular motion. The other problem

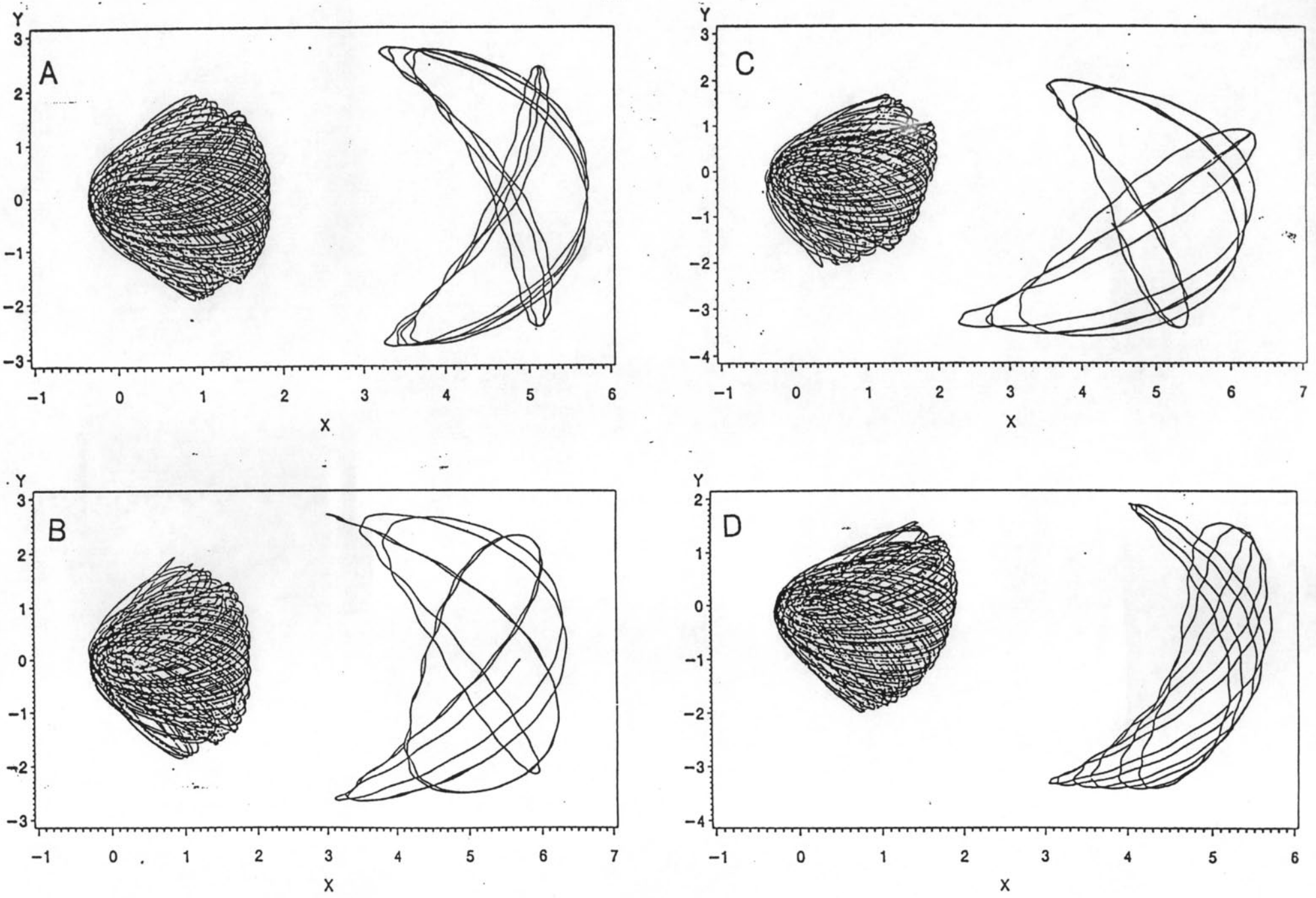


Figure 3. Trajectory plots for different values of dR/dt and dα/dt. R=6.0, α=0.1π. The nucleus is located at (0,0). (a) dR/dt=0, dα/dt=0; (b) dR/dt=0, dα/dt=0.05; (c) dR/dt=0.1, dα/dt=0; and (d) dR/dt=0.1, dα/dt=0.05.

with this model is that it will not produce correct results for the motion of the outer electron, if the inner electron is frozen.

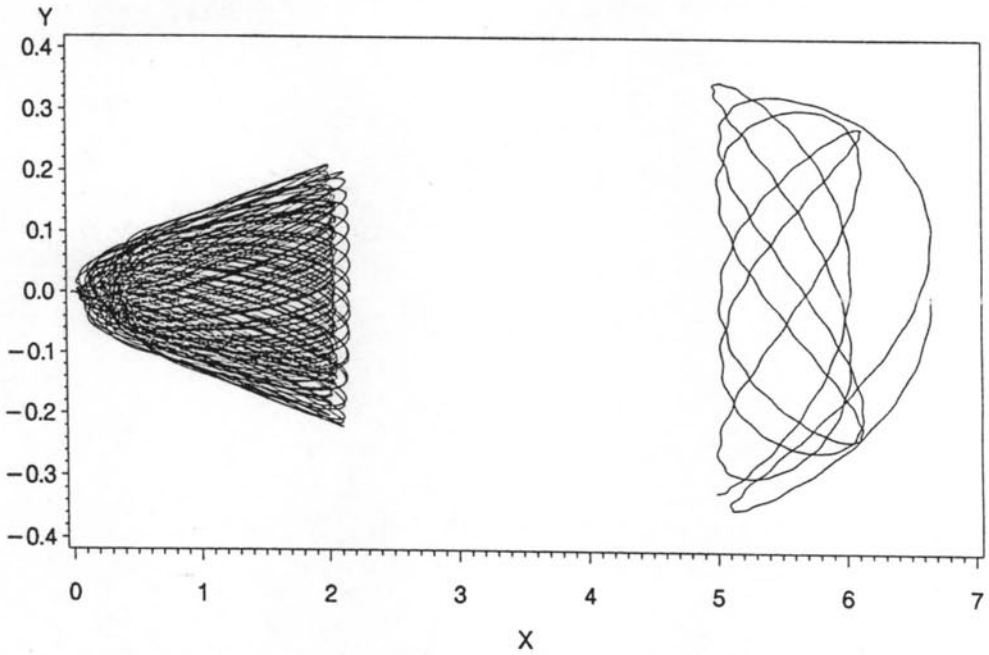


Figure 4. Illustration of a torus-filling trajectory.
Initial conditions: R=7, dR/dt=0, α=0.1001π, dα/dt=0.

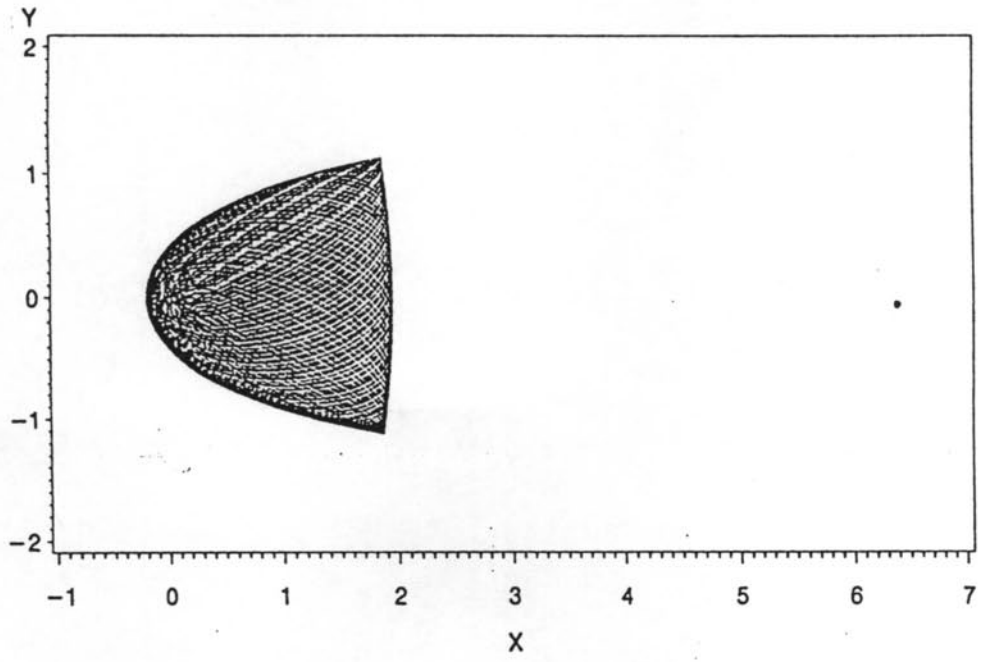


Figure 5. Illustration of a trajectory using the frozen planetary approximation.

II.3 Frequency Analysis

Instead of plotting the trajectories in Cartesian coordinates, it is also

useful to plot various quantities of the system as they evolve over time. When this is done several relationships appear in the various physical properties of the system. In essence, there are six quantities which are useful to observe over time: the angle to the Runge-Lentz vector, the angle to the outer electron, the difference in these two angles, the radial position of the outer electron, the eccentricity of the inner electron's ellipse, and the angular momentum of one of the electrons. Since the total angular momentum is required to be zero, it is unnecessary to view the angular momentum of both electrons. The Runge-Lentz vector is, in essence, the major axis of the ellipse as shown below. All angles are measured relative to some arbitrary zero.

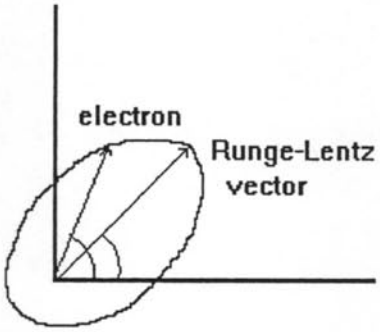
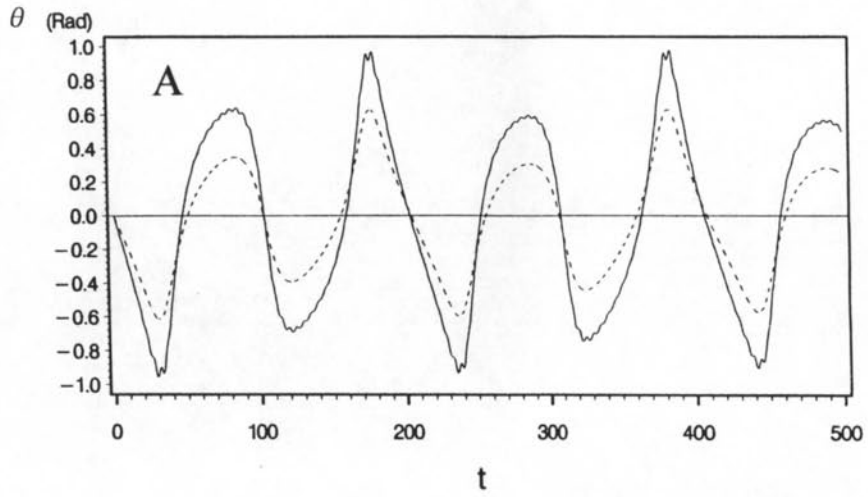


Figure 6. Illustration of Runge-Lentz vector.

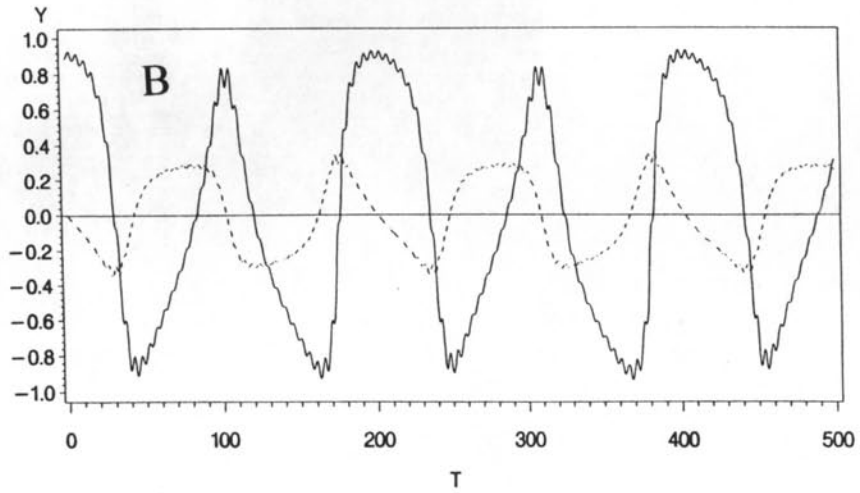
For a trajectory similar to that shown above ((a) of figure 3) these various quantities are plotted versus time in figure 7. It is immediately apparent that the Runge-lentz vector and the outer electron are in a 1:1 phase-locked relationship. Furthermore, the Runge-lentz vector sweeps out a larger angle than the outer electron, confining the outer electron angularly so that stability can be maintained. All of the quantities examined are periodic for this orbit, and others similar to it. Additionally, there are other phase-locking relationships found in the other measurements.

II.4 Stability plots

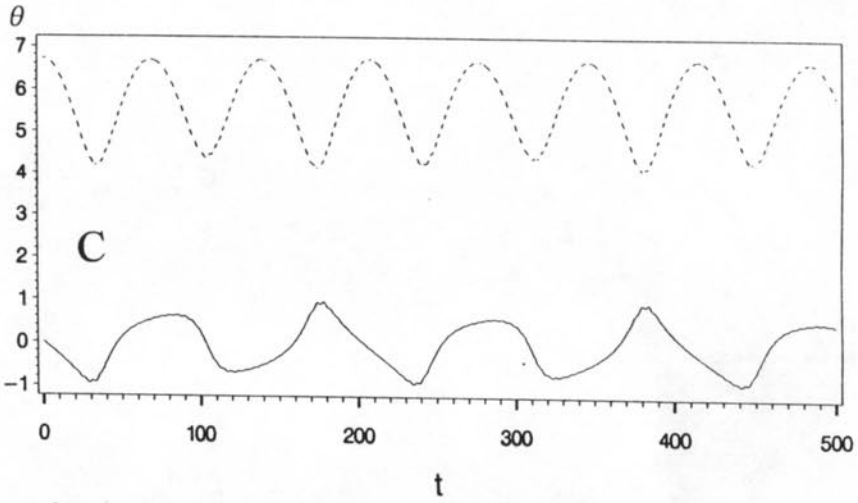
An easy method for getting an overview of the phase space is to make stability studies of the orbits. For these, a large number of initial conditions are run in a grid pattern, keeping two of the four initial conditions fixed. The computer runs each set of initial conditions for a specified time (much longer than the period of any of the quantities involved) and categorizes the orbit as: stable, classically forbidden, or autoionizing. In a stable orbit, the two electrons are still bound to the nucleus after the computer program has numerically integrated the system of equations for some pre-determined



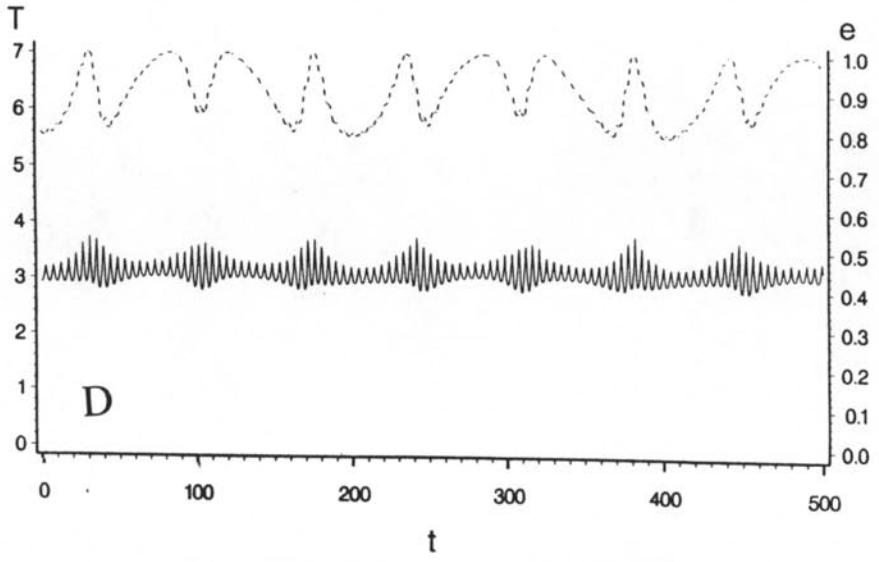
a. Time dependence of the angle to the outer electron (dahed line) and the angle to the Runge-Lentz vector (solid line.)



b. Angular momentum (solid line) and the difference between the two angles in (a) (dashed line.) Note that each curve passes through zero when the other has an extremum.



c. The angle to the Runge-Lentz vector (solid line) and the radial position of the outer electron (dashed line) plotted on the same scale.



d. The ellipse of the inner electron: period (solid line) and eccentricity (dashed line.) For torus-filling orbits, this line is virtually flat, just below 1.

Figure 7. The time-dependent quantities for a helium planetary trajectory. Initial conditions: R=7, dR/dt=0, $\alpha=0.8275\pi$, $d\alpha/dt=0$.

period of time, T_c. A classically forbidden orbit is not a true orbit, since, in order to use the specified initial conditions, the time derivative of q would initially be imaginary. The autoionizing orbits are broken down into inner and outer autoionization, based on which electron is no longer bound to the nucleus. For each of these orbits, one of the electrons is ejected, heading off to infinity, at some time $t<T_c$. A number of stability plots are given in the appendix.

All of the stability plots exhibit a fractal nature, the structure of which is dependent on the two fixed coordinates and the nuclear charge. The most surprising feature of the plots for helium (Z=2) is the large size of the stable region. Since there are a number of seemingly delicate balances among the frequencies describing the system's motion, one would expect a smaller stable region to reflect the number of initial conditions which could satisfy those balances. Figure 1 in the appendix shows a highly detailed close-up of the stability plots for Helium.

The size of the region of stability does depend greatly on the nuclear charge. Somewhere between Z=3 and Z=4 the stable region shrinks so that it is only a narrow strip running the perimeter of the classically allowable trajectories. Figure 2 in the appendix illustrates the various stability plots for $2<Z<5$. On the other hand, as Z decreases, the stable region splits off, close to Z=1.3, forming two separate stable regions, which are clearly separated by an unblemished region of initial conditions which lead to the autoionization of the outer electron. Using a charge of Z=1.0 is unphysical, since the electrostatic force on the outer electron would be almost completely masked by the inner electron, causing all orbits to autoionize. The plots for $1.1<Z<2$ are given in figure 3 of the appendix.

The splitting can possibly be explained by the existence of two separate types of stable orbits as described above. The torus-filling types can be found just along the boundary between the stable and classically forbidden regions. The existence of these two types of stable orbits has profound consequences for the effective potential in which the electrons move. The determination of this potential will be discussed in section III.

Stability plots of the FPA trajectories show the same intrinsic shape as those for the full Hamiltonian. However, the entire region of physically

allowable coordinates leads to stable orbits as seen below. This is to be expected, since, without the motion of the outer electron, the inner electron moves in a steady potential, with the nuclear attraction dominating. This leads to the usual Kepler ellipses which orbit the nuceus and are perturbed by the steady state field of the outer (fixed) electron.

II.5 Poincare Surfaces

Another method of studying the overall stability of a given orbit is by the method of Poincare sections. This method only works properly when the phase space being studied is four dimensional. One then creates a two-dimensional picture by only looking at points on the orbit where one of the three variables has a given value. Then, by noting whether the orbit makes a closed loop, a series of closed loops or scattered, unconnected points, one can determine whether the orbit is stable, periodic, resonant, or completely unstable.

In the current problem, we have several complications for using this method which make it less useful than in other instances. First, the phase space is six dimensional. This means that the surface of section at constant energy can only reduce the number of variables from five to four. Viewing a four-dimensional surface is impossible, and applying any of Poincare's methods to identifying the type of orbit can not be done. Thus, we must take "thin slices" in the other coordinates, effectively taking multiple Poincare surfaces at once. This can reduce the problem to two dimensions and allow the resulting surface of section to be analyzed if there are enough data points left after "slicing" to form any coherent structure. This is not always posible.

The second problem with this method involves calculating the enormous number of data points needed. Once a method has been determined to reduce numerical error and produce "good" points on the surface, the problem of actually calculating these points is computer-intensive, requiring a great deal of time for one orbit. Since this method works best when applied to multiple orbits, allowing the production of several, overlayed surfaces of section, the computer time necessary is prohibitive.

The third major problem with the method of sections is that of the aforementioned numerical error. It is relatively easy, using these techniques for a small error in rounding or some other function to magnify, destabilizing a particular orbit, causing the data points to wander off of the previously well-defined surface of section.

It is, however, possible to overcome these difficulties using the method of "analytic shooting." This method involves treating the inner electron as if it moves on a perfect ellipse in a central potential modified by the effects of the outer electron. When the inner electron reaches a point where energy conservation becomes a problem, analytic shooting moves the electron through the to point on the ellipse which is stable. Since the inner electron revolves around the nucleus much faster than the outer electron moves, one can simply treat the outer electron as continuing in its present trajectory for the time necessary for inner electron to move to its new position. After taking a surface of section with $\theta_{12}=0$ (that is, when both electrons are in conjunction with the nucleus) and then taking thin slices in the other coordinates, the following surface of section can be produced, after scaling.

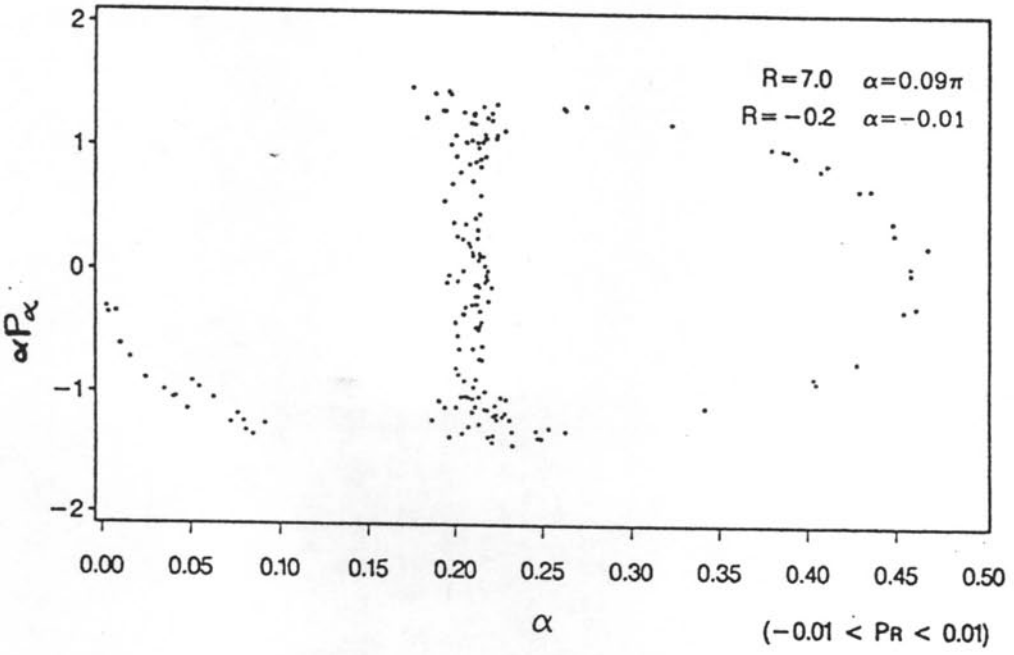


Figure 8. Surface of section for helium. Note the two separate islands indicating a resonance.

This graph shows the coordinates $P\alpha$ versus α and has been cropped to eliminate some of the erroneous data created by numerical error. The existence of two islands for a single set of initial conditions clearly predicts

the existence of strong resonances, as seen in the frequency analysis of this orbit.

Using these surface of section plots, one can calculate the quantum numbers associated with the trajectory by calculating the areas enclosed by the orbits on the surface. However, it would take a great deal of time to calculate one orbit, much less the many necessary for correct quantum predictions. This is the primary reason that calculations of this type were not used extensively, although they could greatly aid the development of a full description of the planetary states of helium.

III. Results

III.1 The Stark Frequency

Examination of the trajectories generated by the FPA approximation suggests that the inner electron's motions are governed by the Stark Effect caused by the electric field of the outer electron. The Stark Frequency can be calculated by the application of

$$\omega_s = \frac{3}{2} n^2 \frac{\overline{E_{elec}}}{Z}$$

This expression can be simplified by using the quantum mechanical definitions of the inner electron's radial position.

$$r_i = \frac{3}{2} \frac{n^2}{Z}$$

Due to scaling,

$$E \equiv \frac{Z^2}{2n^2} E_0$$

where

$$E_0 = -1$$

and thus the scaling invariance gives

$$r_i' = \frac{2n^2}{Z^2} r_i$$

leading to

$$r_i = \frac{3}{4} Z$$

The classical expression of the electric field due to the outer is electron is

$$E_{elec} = \frac{1}{(r_o - r_i)^2}$$

In these expressions, r_i and r_o represent the radius of the innner and outer electron, respectively. Combining these expressions, we get a simple equation for the Stark frequency.

$$\omega_s = \frac{3/4 Z}{(r_o - 3/4 Z)^2}$$

Further, we can empirically estimate the outer electron's radial position from the computer plot of the trajectories. The table below shows the average radius over a trajectory of fixed time for each electron at different values of Z. Note that the table also shows the maximum and minimum values for α that can be used as initial conditions for the orbit. All trajectories have the following initial conditions:

$$R = 7.0 \qquad dR/dt = 0.0 \qquad d\alpha/dt = 0.0$$

The average radii were all calculated for the upper value of α. These orbits fall along the edge of the stable region and are of the torus-filling variety. The maxmum and minimum radii shown are the radii for the outer electron for initial conditions leading to a near-autoionization, ie these points are the result of trajectories whose intitial conditions used the lower bound for α.

The graphs below illustrate the values shown in the table. The minimum and maximum values of α can be estimated by linear functions of Z, as can the average radius of the inner electron. The average radius for the outer electron can be approximated by the form (with E=-1)

$$r_o = \frac{0.5}{(Z-1.2)^2} + 3.5 + 0.9Z$$

Z	α(min)	α(max)	<Rin>	<Rout>	R(min)	R(max)	θ(max)	Δθ(max)
1.3	0.034	0.060	0.973	8.583	1.737	13.753	1.80	1.50
1.4	0.041	0.065	1.062	7.053	2.068	8.659	0.90	0.88
1.5	0.047	0.070	1.139	6.438	2.273	7.810	0.95	0.80
1.6	0.052	0.076	1.227	6.162	2.144	13.214	1.70	0.80
1.7	0.059	0.082	1.325	6.086	2.418	7.855	0.85	0.65
1.8	0.070	0.088	1.412	5.987	3.024	6.952	0.70	0.55
1.9	0.068	0.094	1.501	5.938	2.362	14.610	0.85	0.65
2.0	0.083	0.100	1.589	5.918	3.005	10.024	1.05	0.45
2.1	0.088	0.106	1.655	5.851	2.281	17.364	0.75	0.45
2.2	0.098	0.112	1.777	5.930	3.738	6.992	0.80	0.35
2.3	0.103	0.118	1.871	5.975	3.667	6.952	0.95	0.40
2.4	0.110	0.124	1.959	5.990	3.900	7.180	0.80	0.30
2.8	0.138	0.150	2.357	6.378	4.770	7.409	0.60	0.30
2.9	0.137	0.156	2.455	6.514	2.927	10.105	0.90	0.40
3.0	0.145	0.161	2.533	6.600	4.414	11.131	0.92	0.35

Table 1. Showing the values measured and computed for several values of Z. The values Z=2.5,2.6,2.7 were rejected due to numerical error. The radii and α information is shown graphically below.

Calculating the Stark frequency for Z=2 by this method gives numbers which agree reasonably well with the obseved values in the computer program. For example, at Z=2, $\langle r_0 \rangle$=6.08 (by the formula given above) and, thus, ω_S=0.07, predicting a period of about 90 units of scaled time. Looking at the graph shown in figure 7(a), one can see that the orbit completes one oscillation in slightly less than 100 units of time.

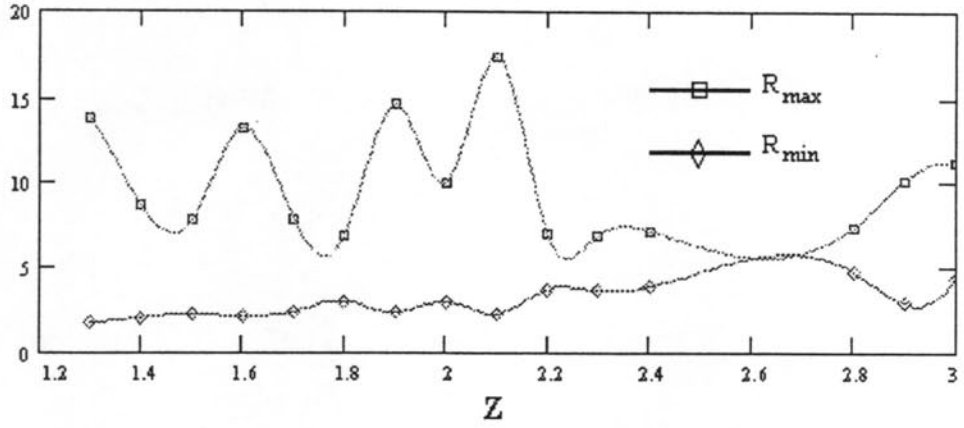


Figure 9. Graph showing observed maximum and minimum radii for the outer electron. The intitial conditions used were: R=7, dR/dt=0, $d\alpha/dt=0$, and the lower bound of α for each value of Z.

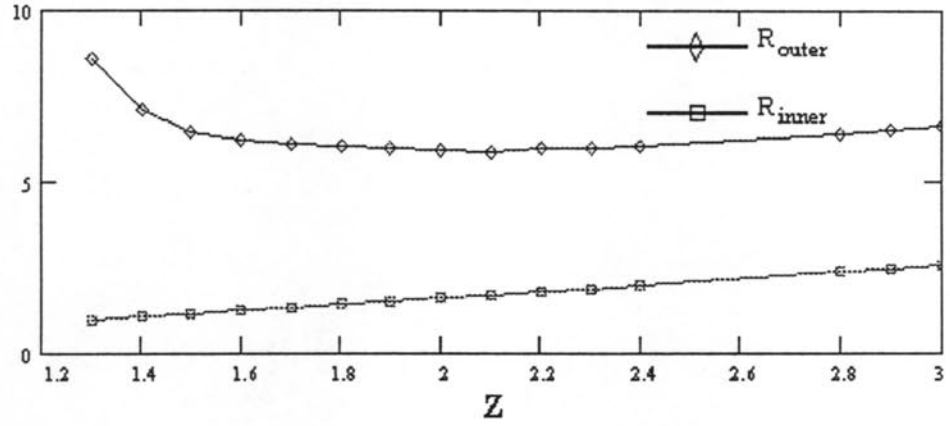


Figure 10. Graph showing Z dependence of the average radii for the inner and outer electron. The intitial conditions used were those for a torus-filling trajectory, along the upper bound of α.

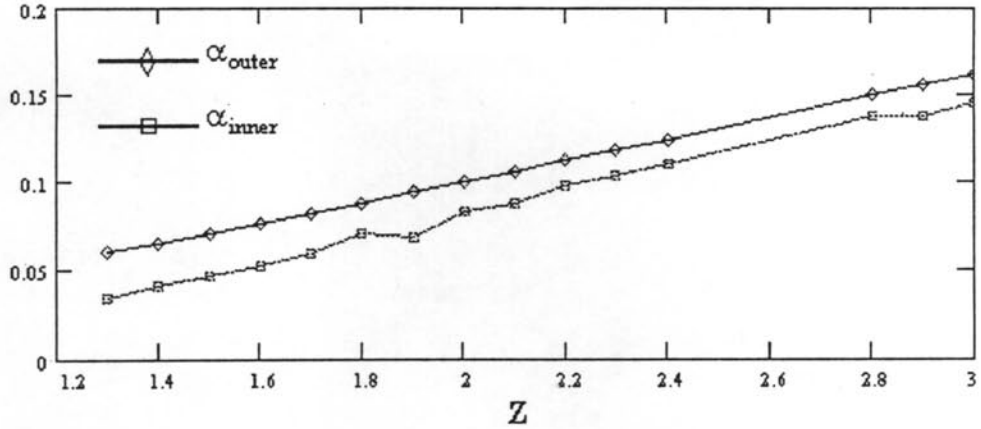


Figure 11. Graph showing boundary values of α for different values of Z. When α falls outside these values, all orbits tend to autoionize.

III.2 Quantum Numbers

It is possible to estimate the quantum regime in which planetary states lie by use of the information in the table above. Normally, the quantum state for a two-electron atom can be described interms of the quantum numbers of each electron: n_i, l_i, m_i. This discription is usually given in terms of n_1, n_2, l_1, l_2, L, and M, where L, and M are the total angular momenta. However, for these planetary states, we have chosen L=0. This forces M=0 and l_1=l_2. Thus, the system can now be described using only three quantum numbers: n_1, n_2, l.

A better method for describing these states is given by the following three quantum numbers. It is beyond the scope of this paper to discuss why these numbers are any better then the others.

$$n = \max(n_1, n_2)$$
$$N = \min(n_1, n_2)$$
$$K \approx -N\cos(\Theta_{12})$$

These quantum numbers can be estimated from the quantities in table 1 by the following formulae. In these, r_i corresponds to the average radius of the inner electron reported in table 1. The variables r_{max} and r_{min} represent the maximum and minimum observed values of the radius of the outer electron. The quantity $\Delta\theta_{max}$ refers to the maximum difference in the angle between the Runge-Lentz vector and the angle to the outer electron. This is measured at near-autoionization.

$$\sqrt{\frac{r_i Z}{r_{max}(Z-1)}} < \frac{N}{n} < \sqrt{\frac{r_i Z}{r_{min}(Z-1)}}$$

$$\frac{K}{N} > -\cos(\Delta\Theta_{max})$$

The results of these calculations are summarized in the table below and shown graphically in the two figures following the table. The defintion of the quantum numbers forces n to be greater than or equal to N. Thus, any

values of N/n greater than 1 have been treated as equal to 1. From the graphs one can see that N/n has a value between 0.5 and 1. This leads to the conclusion that planetary states can only be found in regions where $N \le n < 2N$.

Z	N/n (min)	N/n (max)	K/N
1.3	0.554	1.000	-0.071
1.4	0.655	1.000	-0.637
1.5	0.662	1.000	-0.697
1.6	0.498	1.000	-0.697
1.7	0.640	1.000	-0.796
1.8	0.676	1.000	-0.853
1.9	0.466	1.000	-0.796
2.0	0.563	1.000	-0.900
2.1	0.427	1.000	-0.900
2.2	0.683	0.934	-0.939
2.3	0.690	0.950	-0.921
2.4	0.684	0.928	-0.955
2.8	0.704	0.877	-0.955
2.9	0.609	1.000	-0.921
3.0	0.584	0.928	-0.939

Table 2. Quantum regime of planetary states for various values of Z.

The value of K/N can be approximated by the following formula

$$\frac{K}{N} = \frac{0.1}{Z - 1.2} - 1$$

which tends to -1 as Z approaches infinity. The boundary values of N/n can be approximated using the linear functions:

$$\left(\frac{N}{n}\right)_{\max} = -0.05Z + 1.077$$

$$\left(\frac{N}{n}\right)_{\min} = 0.031Z + 0.543$$

Thus, these simple approximations (ignoring the oscillations in the values of N/n) show that the region of allowable N/n and K/n shrinks with increasing Z, as expected.

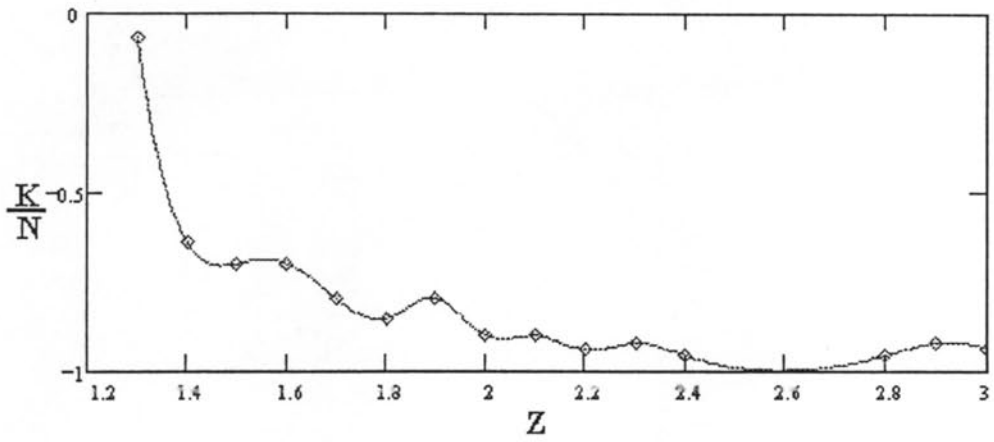


Figure 12. Graph of K/N versus Z.

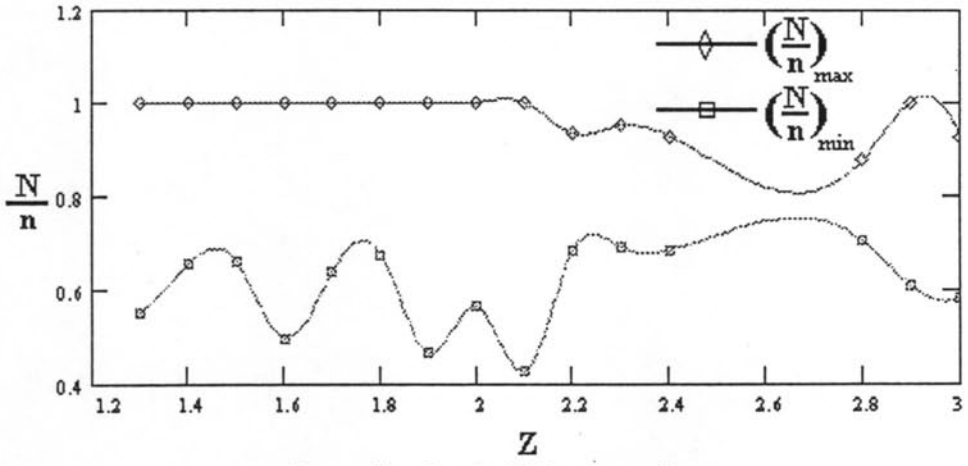


Figure 13. Graph of N/n versus Z.

III.3 The Effective Potential

Another important quantity that can be used in the description of the planetary states is the effective potential for the inner electron. Calculation of this is relatively straightforward, to zeroth order. Like all classical systems, one can approzimate the effective potential as that of the harmonic oscillator:

$$V_{eff} \cong \frac{1}{2}\omega_s \theta^2$$

Where ω_S is the Stark frequency and θ is the angle to the Runge-Lentz vector. However, observations of the trajectories lead one to believe that there is some critical angle, θ_{max}, that bounds this potential. If the Runge-Lentz vector exceeds this angle, the trajectory proceeds to autoionize. Since

$$\theta^2 \approx 1 - \cos^2\theta = \sin^2\theta$$

we can treat the effective potential as

$$V_{eff} = \frac{1}{2}\frac{\omega_s}{a^2}\sin^2(a\theta)$$

where "a" is a parameter which is seen to vary with Z, the nuclear charge. The effective potential is shown below. Plotted along with this is the potential for the harmonic oscillator.

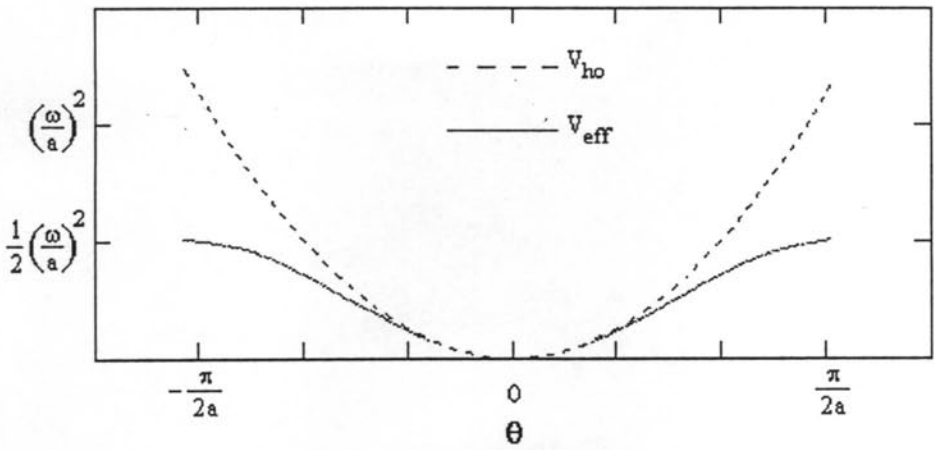


Figure 14. The effective poential.

The maximum for the effective potential is reached when the argument of the sine function is $\pi/2$ or $-\pi/2$. Thus,

$$a = \frac{\pi}{2\theta_{max}}$$

The value of "a" can be determined from the maximum values of θ at break up. These are listed in Table 1. The graph in figure 15 illustrates the Z dependence of "a." Figure 16 shows θ_{max} as a function of Z. The value of "a" should diverge with increasing Z, but there are not enough data points to support this.

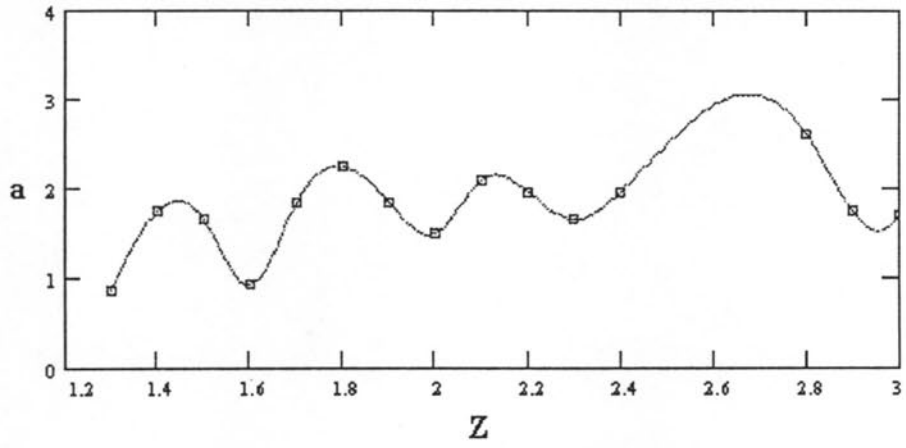


Figure 15. The value of the constant 'a' in the effective potential as a function of Z.

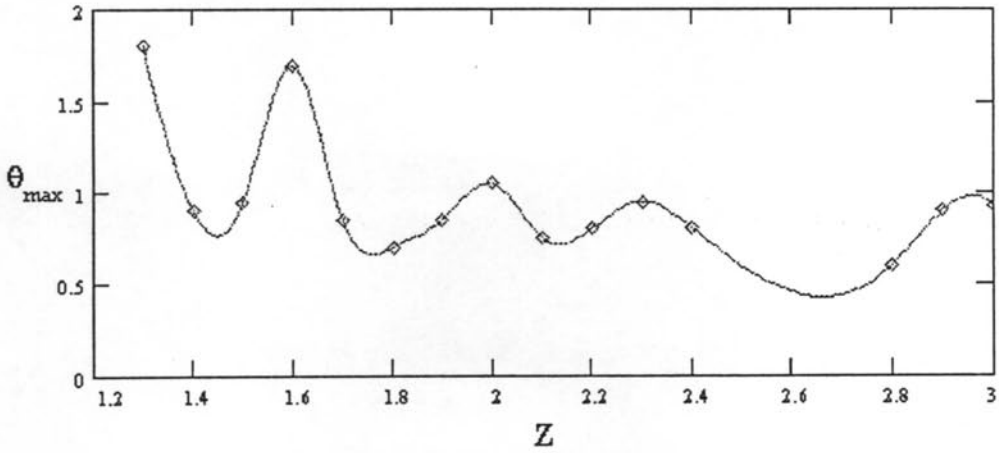


Figure 16. Graph of θ_{max} versus Z at near-autionionizing trajectories.

References

J.Mueller, J. Burgdoerfer, and D. Noid, Phys. Rev. A **45**, 1471 (1992).

K. Richter, G. Tanner, and D. Wintgen, Phys. Rev. A **48**, 4182 (1993).

K. Richter and D. Wintgen, Phys. Rev. Letters **65**, 1965 (1990).

K. Richter and D. Wintgen, J. Phys. B: At. Mol. Opt. Phys. **23**, L197 (1990).

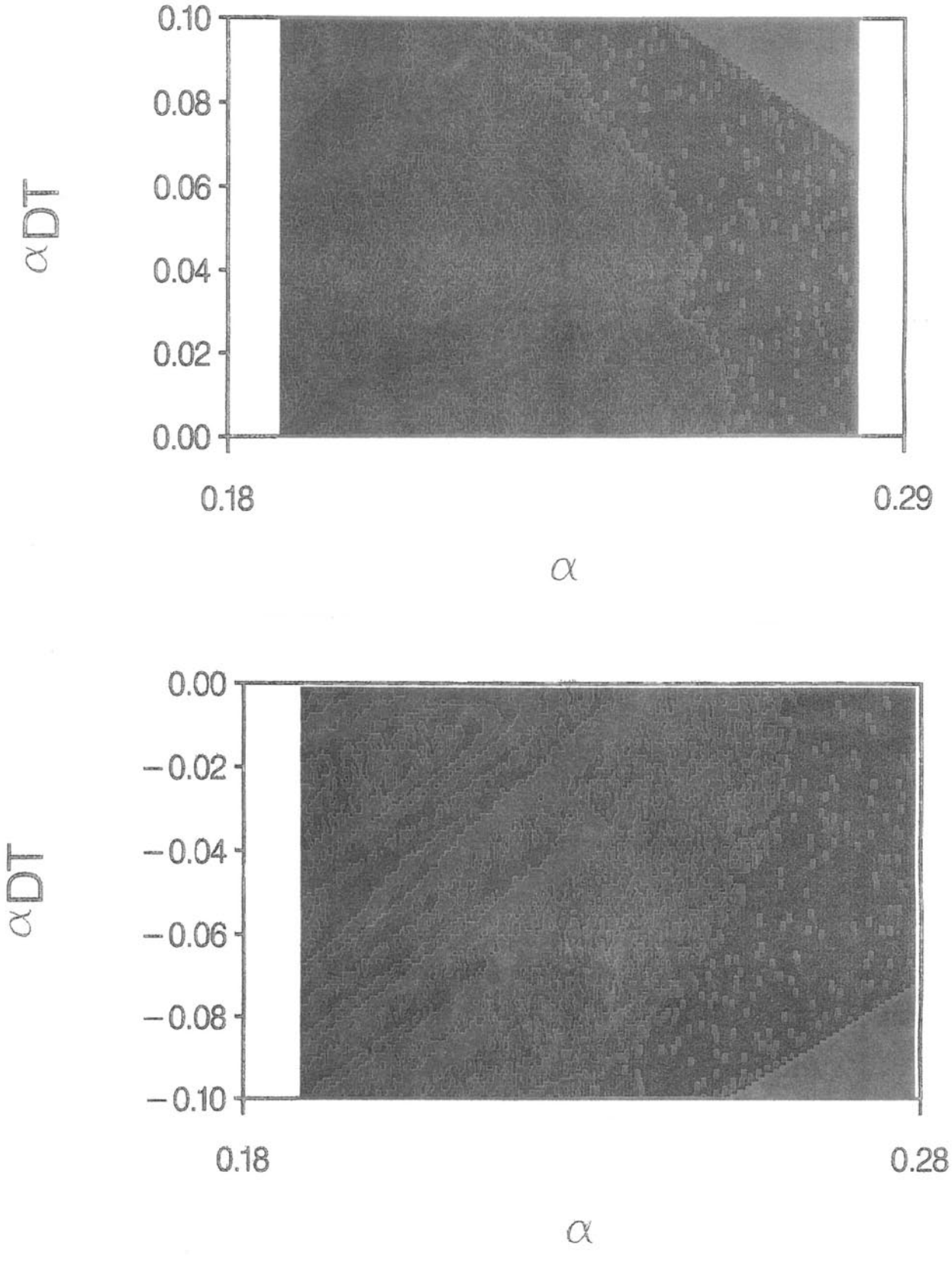
T. Yammamoto and K.. Kaneko, Phys. Rev. Letters **70**, 1928 (1993).

Appendix

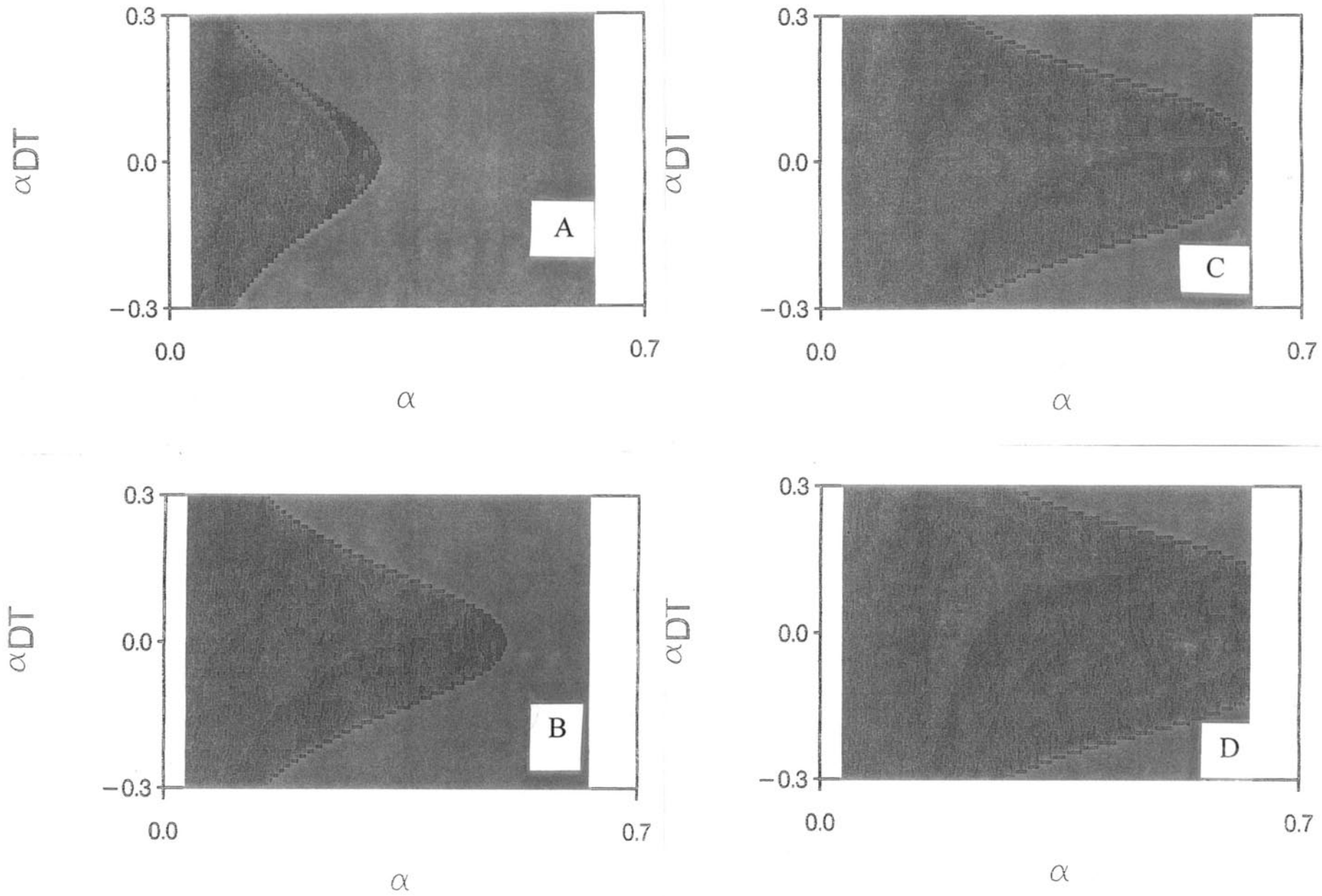
The following pages illustrate the stability plots discussed in the body of the paper. In each, the following initial conditions are constant:

$$R = 7.0 \qquad dR/dt = 0$$

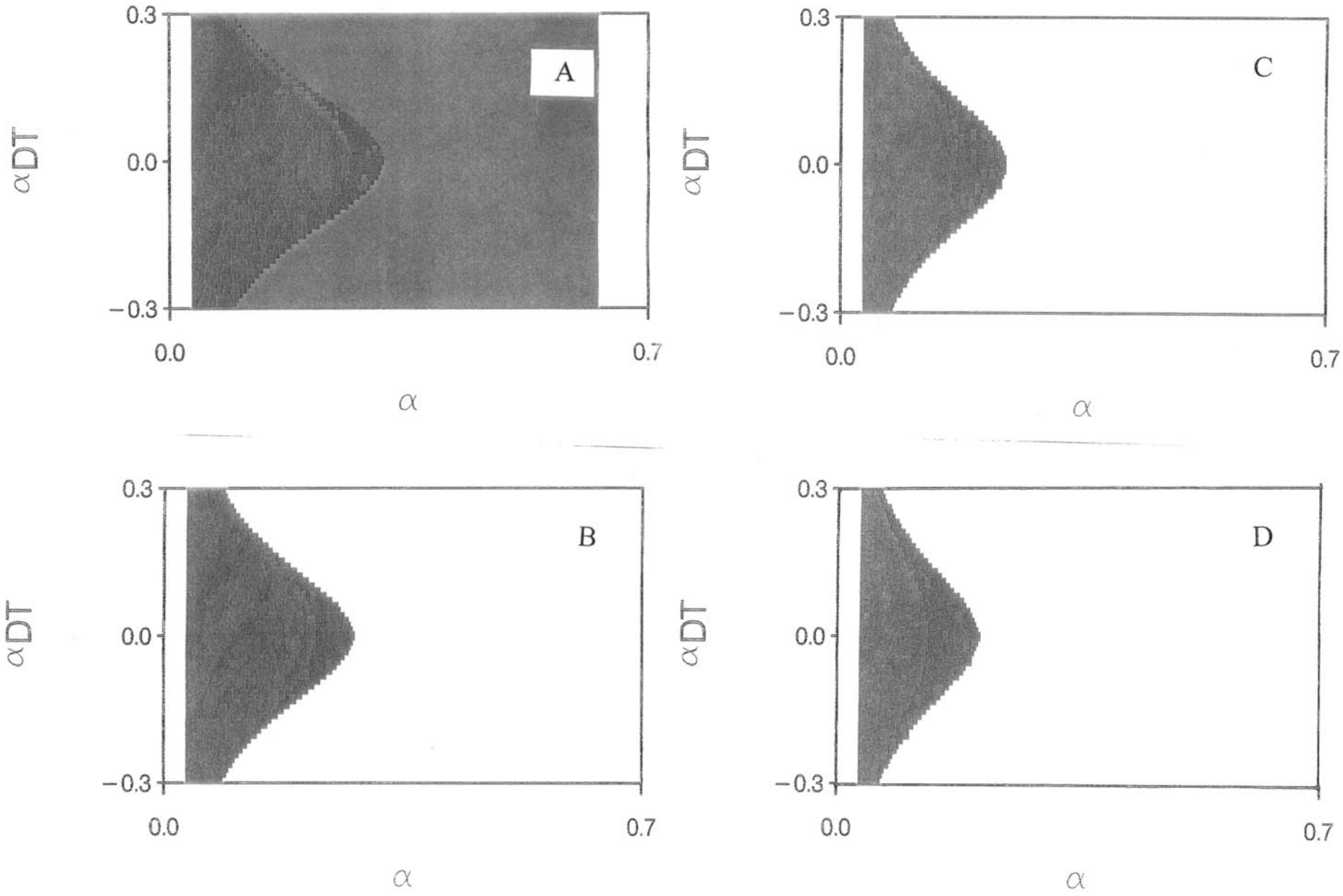
Each of the graphs is plotted in $d\alpha/dt$ versus α, where these are the other two intitial conditions for the orbit. For the pictures, a given set of initial conditions is marked in red to indicate that it is stable. Blue points indicate initial conditions leading to the ejection of the inner electron. Green points mark autoionizing orbits which eject the outer electron. Black or white points are used to mark classically forbidden sets of initial conditions. Inside the stable regions are a number of randomly scattered blue points. These are the result of numerical instabilities in the computer program.



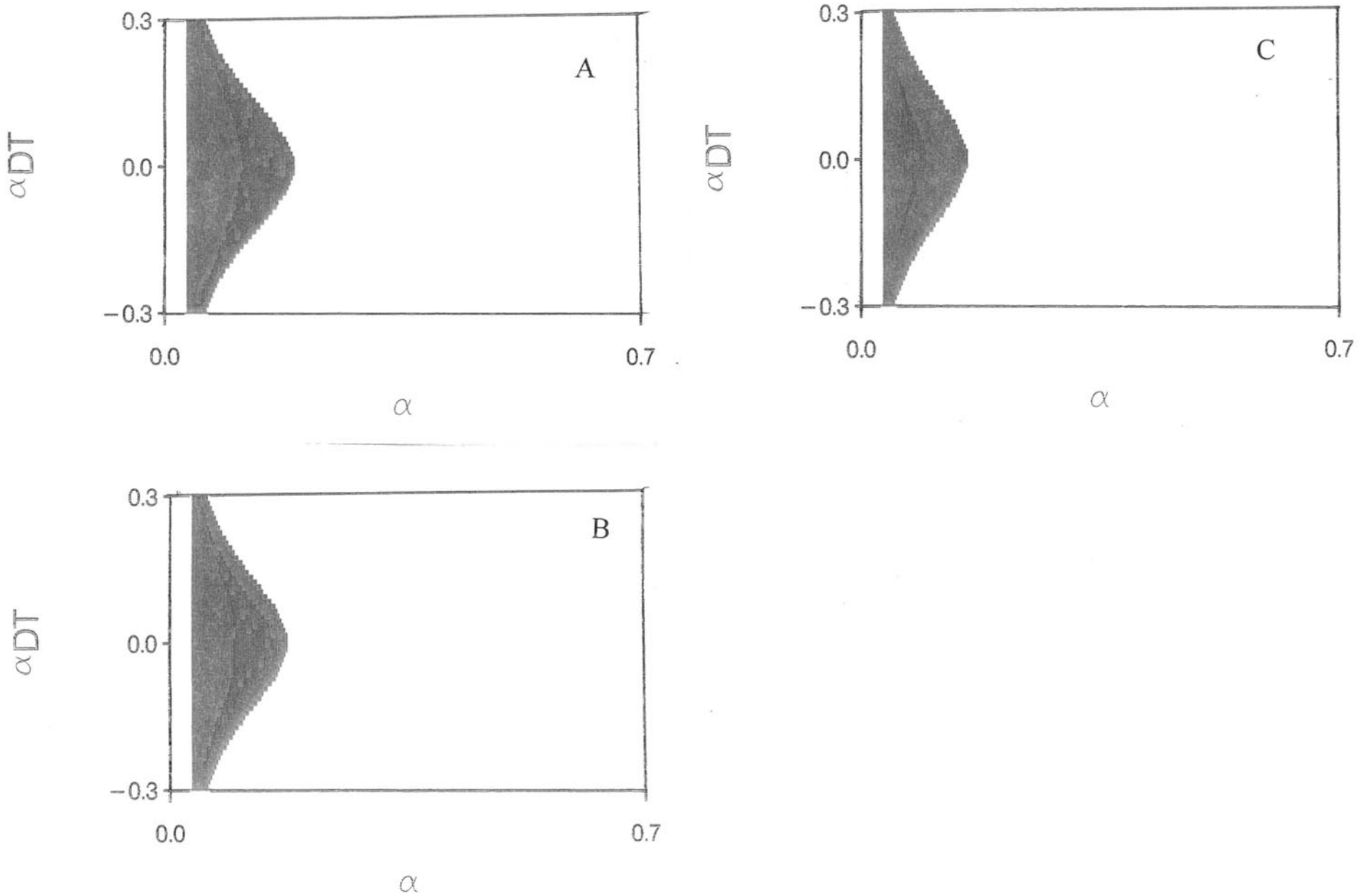
Appendix Figure 1. Stability plot close-ups for Z=2.



Appendix Figure 2. Stability plots for (a) Z=2, (b) Z=3, (c) Z=4, and (d) Z=5. Note the "thinning" out and eventual disappearance of a stable region.



Appendix Figure 3.1. Stability plots for (a) Z=2, (b) Z=1.8, (c) Z=1.6, and (d) 1.4.



Appendix Figure 3.2. Stabililty plots for (a) Z=1.3, (b) Z=1.2, and (c) Z=1.1. Note the splitting of the stable region into a thin strip on the edge and a larger region on the interior.